

## *Near-infrared spectroscopy: rapid and effective tool for measuring fructose content*

**Keywords:** Fructose (fruit sugar), sugars, °Brix, NIR-spectroscopy (near-infrared), adverse physiological effects of fructose, metabolic disorder, cardio-vascular diseases, pre-treatment of spectra, valence vibration, harmonic vibration, statistical spectra analysis

### 1. SUMMARY

Since high fructose intake was found to be associated with increased health risks, it is important to raise awareness towards the amount of this widely used sugar within foods and beverages. The rapid and accurate detection and quantification of sugar types is not an easy task using conventional laboratory technologies. Near-infrared (NIR) spectroscopy has been proven to be a useful tool in this regard, and the present study highlights the applicability of this rapid correlative analytical technology in the measurement of fructose concentration against that of other sugars in aqueous solutions of sweeteners. The presented NIR calibrations are accurate for the relative measure of °Brix ( $R^2 = 0.84$ ), and the direct measurement of the individual sugars ( $R^2 > 0.90$ ) even in solutions with multiple sugars.

<sup>1</sup> Department of Nutritional Science and Production Technology, Faculty of Agricultural and Environmental Sciences, Szent István University, Kaposvár Campus

<sup>2</sup> Department of Physics and Control, Faculty of Food Science, Szent István University, Budapest Campus

<sup>3</sup> Adexgo Kft., Balatonfüred, Hungary

\* Corresponding author: [bazar@agrilab.hu](mailto:bazar@agrilab.hu)

**Haruna Gado YAKUBU**  
**Zoltán KOVÁCS Dr.**  
**Flóra VITÁLIS**  
**György BÁZÁR Dr.**

[harunagado12@gmail.com](mailto:harunagado12@gmail.com)  
[kovacs.zoltan.food@uni-mate.hu](mailto:kovacs.zoltan.food@uni-mate.hu)  
[vitalis.flora@gmail.com](mailto:vitalis.flora@gmail.com)  
[bazar@agrilab.hu](mailto:bazar@agrilab.hu)

<https://orcid.org/0000-0002-9606-7140>  
<https://orcid.org/0000-0003-0641-8830>  
<https://orcid.org/0000-0002-4198-2202>  
<https://orcid.org/0000-0001-9829-4366>

## 2. Introduction

Food sweeteners have become the most widely used additives in the food processing industry, especially in the production of beverages and other products such as desserts and yoghurts. One of the oldest sweetener to have been documented in history is honey [1]. This, and some of the traditional sweeteners such as maple syrup, carob, and agave, consumed for decades are largely made up glucose, fructose, sucrose, minerals and other compounds [1]. Glucose is almost always present in foods and plays an essential role in the regulation of metabolism in human. It can be ingested either as free available sugar (glucose powder) or bonded in polymers, in the case of starch, dextrin, and maltodextrins. Glucose could also be bonded in disaccharides, like in the case fructose bond to glucose in sucrose [2].

For some time now, concerns about the form and levels of sweeteners used in the food industry, and the °Brix value of processed foods, have been topical due to the health implications of the consumers. This is mainly because of the risk of developing metabolic abnormality (diabetes) associated with high intake of sugar, especially sugar of high fructose content. Consumers are therefore becoming more conscious of what they consume, and will at times prefer a reduction of the caloric levels of processed foods, consequently reducing sugar intake [3].

High fructose intake was found to be associated with a high risk of metabolic syndrome [4], obesity, diabetes and an increase in blood triglyceride concentrations and insulin resistance compared with high glucose intake [5], [6], [7]. High risk of cardiovascular diseases and even malignant tumors in body tissues may be related to excessive fructose intake [8], and also dyslipidemia and kidney diseases [9].

Over the years, the application of near-infrared spectroscopy (NIR) to analyze the forms of sugar in food sweeteners, has been found to be easier, faster and cost-efficient [10] compared with tedious and reagent involving methods, such as gas chromatography (GC), high-performance liquid chromatography (HPLC) and enzymatic analysis [11], [12]. The HPLC is the most frequently used method for assessing free fructose, free glucose, sucrose, maltose, and lactose content [13].

The NIR spectral region is found between 800 to 2500 nm ( $12500\text{--}4000\text{ cm}^{-1}$ ) range, with absorptions representing overtones and combinations which are associated with  $\text{--CH}$ ,  $\text{--OH}$ ,  $\text{--NH}$ , and  $\text{--SH}$  functional groups [14]. In the case of glucose, 1st overtone of O–H stretching corresponds to absorption bands at 1195, 1385, 1520, 1590, 1730 nm, 1st overtone of O–H stretching of fructose and sucrose at 1433 nm, and O–H combination band of sucrose, glucose and fructose at 1928 nm [14].

Mono- and disaccharides, such as glucose, fructose, sucrose, lactose, were also analyzed in aqueous solutions [15]. Although the same molar concentrations of all the concerned sugars were dissolved, the mass that those represented differed considerably due to the differences in molecular weights of mono- and disaccharides. When quantifying sugars in mixtures, the molar concentration of the sugar solutions gave less accurate calibration models compared with those fitted on weight per volume concentration. Since the spectral information is mostly the light absorbance of chemical bonds during excitation, this information is more proportional with the number of chemical bonds and atoms in the aqueous solution, than with the number of molecules. Regression coefficient vectors of calibration models for each of the sugars also revealed the spectral regions holding the highest importance in the quantitative analysis of the sugars. Regression vectors of the 1100-1800 nm interval, associated with signals of O–H and C–H bonds, showed the significance of characteristic spectral regions of water and the dissolved sugars. The calibration on the concentration of the sugars within the mixtures showed accurate validation performance even at low concentration levels ( $0.0018\text{--}0.5243\text{ g/cm}^3$ ),  $R^2_{CV}$  of 0.841 and 0.961, SECV of  $0.024\text{ g/cm}^3$  and  $0.012\text{ g/cm}^3$  for glucose and fructose, respectively. This showed possible quantification of a specific sugar in a mixture of sugars in a solution using NIR spectroscopy [15].

In related studies [10], [16], [17], glucose, fructose and sucrose were quantified in different fruit juices using NIR, and accurate partial least square regression (PLSR) models were reported ( $R^2 > 0.854, 0.963, 0.953$  for glucose, fructose, sucrose, respectively). Good PLRS models were reported for predicting glucose within 900-2200 nm wavelength range [18], whereas the 900-1650 nm interval was reported to be good for the discrimination of organic sugar and conventional brown sugar using partial least squares discriminant analysis (PLS-DA) models [19]. In a study, the concentration of glucose in an aqueous mixture of glucose, albumin and phosphate was quantified using NIR and reported accurate PLRS models [20]. The possibility to predict the glucose, fructose and sucrose content in *Morinda officinalis* extracts utilizing NIR was also reported [21].

The Hungarian food industry is flooded with many sweeteners for food processing. However, there are three major sweeteners: K-syrup LDX and K-sweet F55, which are two commonly used isosugars, and D-sucrose. K-syrup LDX is a sweet, viscous, quickly crystallizing syrup often used in food and pharmaceutical industry

as a raw material for fermentation. It contains high amount of glucose or dextrose (93%), and small amount of fructose (0.5%) and viscous liquid [22]. K-sweet F55, however, is a high caloric isosugar consisting of glucose and fructose, where the fructose content is higher (55%) than the glucose (45%) [23], and the third sweetener is D-sucrose or refined sugar, which is increasingly being replaced with K-syrup LDX and K-sweet F55.

This study aimed to determine the applicability of NIR spectroscopy to quantify glucose, fructose, sucrose content and °Brix of aqueous solutions of the widely used sweeteners, D-sucrose, K-syrup LDX, and K-sweet F55.

### 3. Materials and Methods

#### 3.1. Sample preparation

Three kinds of sugars were used with brand names: D-sucrose (Carl Roth GmbH, Karlsruhe, Germany): 100% sucrose; K-Syrup LDX (KALL Ingredients Kft., Tiszapüspöki, Hungary): 93% glucose + 0.5% fructose + 6.5% water; K-Sweet F55 (KALL Ingredients Kft., Tiszapüspöki, Hungary): 45% glucose + 55% fructose. Aqueous solutions were prepared at 10 different concentrations for each of the three sugars, separately. A total sample of 30 samples was prepared, 100 ml of each.

#### 3.2. Laboratory measurement

°Brix was measured with Hanna HI96801 Digital Refractometer, and recorded as reference for subsequent NIRS calibrations. Glucose, fructose and sucrose concentration of the respective sugar solutions was calculated based on the mass of sweetener added to the solutions and the percentages of the individual sugars within the sweeteners. The following formulas were used for the calculation of glucose and fructose in K-sweet F55 and K-syrup LDX solutions:

1. Glucose in K-syrup LDX solution =  $93/100 \times \text{amount of K-syrup in solution (g/100g)}$
2. Fructose in K-syrup LDX solution =  $0.5/100 \times \text{amount of K-syrup in solution (g/100g)}$
3. Glucose in K-Sweet F55 solution =  $45/100 \times \text{amount of K-sweet F55 in solution (g/100g)}$
4. Fructose in K-sweet F55 solution =  $55/100 \times \text{amount of K-sweet F55 in solution (g/100g)}$

Accordingly, each of the 30 samples was described with °Brix, and concentrations of total sugar, glucose, fructose and sucrose, as listed in **Table 1**.

Table 1. The °Brix, concentration of total sugar, glucose, fructose and sucrose of the aqueous sugar solutions used for the study

Sweetener	°Brix	Total sugar (g/100g)	Glucose (g/100g)	Fructose (g/100g)	Sucrose (g/100g)
D-sucrose	1.100	1.100	-	-	1.100
	2.000	2.000	-	-	2.000
	2.900	2.900	-	-	2.900
	4.100	4.100	-	-	4.100
	4.900	4.900	-	-	4.900
	6.000	6.000	-	-	6.000
	6.800	6.800	-	-	6.800
	8.200	8.200	-	-	8.200
	9.100	9.100	-	-	9.100
10.10	10.10	-	-	10.10	
K-syrup LDX	0.300	0.373	0.346	0.001	-
	1.000	1.245	1.157	0.006	-
	2.000	2.491	2.316	0.012	-
	2.500	3.110	2.892	0.015	-
	3.400	4.232	3.935	0.021	-
	4.100	5.107	4.749	0.025	-
	4.200	5.232	4.865	0.026	-
	5.500	6.850	6.370	0.034	-
	6.400	7.971	7.413	0.039	-
7.300	9.000	8.370	0.045	-	
K-sweet F 55	0.400	0.420	0.189	0.231	-
	0.700	0.732	0.329	0.402	-
	1.200	1.250	0.562	0.687	-
	1.700	1.779	0.800	0.978	-
	2.500	2.716	1.222	1.493	-
	3.100	3.241	1.458	1.782	-
	3.400	3.558	1.601	1.956	-
	3.900	4.081	1.836	2.244	-
	5.300	5.555	2.499	3.055	-
7.600	7.953	3.578	4.374	-	
Max value	10.10	10.10	8.370	4.374	10.10
Min value	0.300	0.373	0.189	0.002	1.100
Mean	4.216	4.403	2.824	0.871	5.520
SD	2.836	2.841	2.434	1.239	3.055

D-sucrose: 100% sucrose; K-syrup LDX: 93% glucose+0.5% fructose; K-sweet F55: 45% glucose+ 55% fructose; SD: standard deviation; Max: maximum value; Min: minimum value

### 3.3. NIRS measurement

The samples were scanned at room temperature (25 °C) using a FOSS NIRSystems 6500 (FOSS NIRSystems, Inc, Laurel, MD, USA) spectrometer, operated with WinISI v1.5 software (InfraSoft International, Port Matilda, PS, USA). The scanning was done in transmission mode after measuring 1 ml sugar solution into a quartz cuvette having 1 mm pathlength. Two rounds of scanning of each sample were done randomly, and the subsequent sample was used to wash the cuvette three times between each sample scanning. Sixty spectral data were obtained and the spectra of the two rounds were averaged resulting in 30 spectra.

### 3.4. Spectral pre-processing and multivariate data analysis

The Unscrambler v9.7 (CAMO Software AS, Oslo, Norway) software was used for the analysis of the NIR data, while the MS Excel 2013 was used to calculate the descriptive statistics for the variables measured and calibrated for °Brix, glucose, fructose, and sucrose concentration.

For scatter correction of spectra, and to obtain accurate and robust calibration models, several spectral types of preprocessing were performed: standard normal variate (SNV), multiplicative scatter correction (MSC) and gap-segment second derivative (2nd order derivative, gap of 5 data points, segment of 5 data points).

Using multivariate data analyses, both the separation of the solutions prepared with different sweeteners and the calibration on the targeted quantitative parameters was performed. Principal component analysis (PCA) [24] was used to investigate the multidimensional pattern of the spectra data and to identify differences among the three groups of the sweetener solutions. The spectral data within the NIR range (1100-1850nm) were calibrated with the laboratory data as the reference, using partial least squares regression (PLSR) models [24]. The optimum number of latent variables (LV) used for the PLSR modelling was determined by full (leave-one-out) cross-validation, when in a 30-step iterative process each of the 30 samples was left out of the calibration once and was used for validating the model [24].

Evaluation of PLSR models was done by comparing the calibration statistics with that of the cross-validation. The determination coefficient of calibration ( $R^2_c$ ) and cross-validation ( $R^2_{cv}$ ), and the root mean square error of calibration (RMSEC) and cross-validation (RMSECV) were compared, where larger  $R^2$  value and smaller RMSE value represent the better model. During the model optimization processes, RMSECV values were minimized.

## 4. Results and discussions

The recorded raw spectra show the typical NIR absorption of water, with a major peak at 1450 nm, representing the 1<sup>st</sup> overtone region of O–H bond (**Figure 1**). The small peak around 1780 nm represents the 1<sup>st</sup> overtone of C–H bonds. The second derivative spectra were calculated with the gap-segment derivative function, where both gap and segment were set to 5 data points to avoid noise enhancement of the derivative function, still keeping the useful signals within the pretreated data.

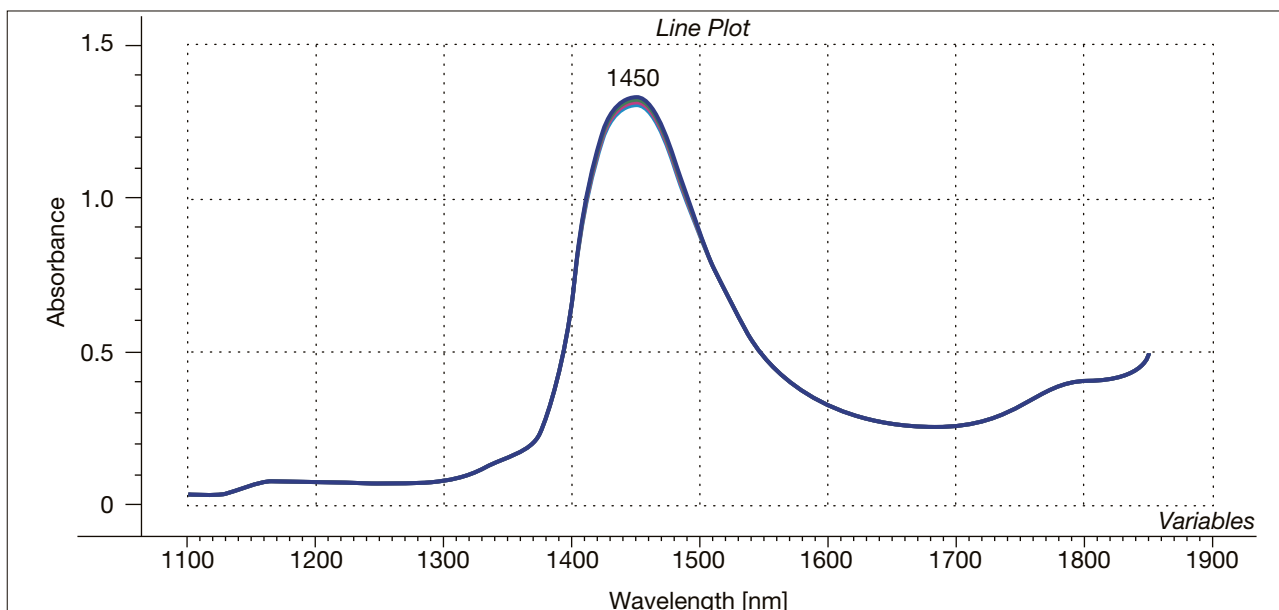


Figure 1. Raw spectra of the sugar solutions in the range of 1100-1850 nm

The negative peaks of the 2<sup>nd</sup> derivative spectra (**Figure 2**) indicate the locations and relative amplitude of the original overlapping absorptions appearing as one in the raw spectra. This shows the well-described phenomenon that major peak of the raw spectrum at 1450 nm is formed by at least two underlying absorptions of water at 1416 nm and 1460 nm, representing less and more H-bonded water, respectively [15].

The applied spectral pretreatments (2<sup>nd</sup> derivative, or SNV, or MSC) did not allow visual differentiation of solutions with different sweeteners, while the gradual changes of the water absorption peaks indicated the effect of the increasing concentration of dissolved sugars on the structure of water [15].

**Figure 3** shows the 3D plot of the PCA performed with 2<sup>nd</sup> derivative spectra of all the 30 solutions. The solutions of the three types of sweeteners are indicated with different colors and numbers. The two plots show the same result from different angles, highlighting that 4<sup>th</sup> principal component (PC4) is responsible for the separation of K-Sweet F55 from D-sucrose and K-Syrup LDX, and PC2 is responsible for the separation of D-sucrose from K-Syrup LDX and K-Sweet F55. Thus, PC2, as new latent variable covering approximately 2% of the variance of the original NIR data, describes the difference between the disaccharide and monosaccharide solutions, while PC4, covering less than 1% of the variance of the original NIR data, describes the difference between the solutions of high fructose syrup and that of the other sweeteners. The combination of PC2 and PC4 describes the differences between glucose solutions and others.

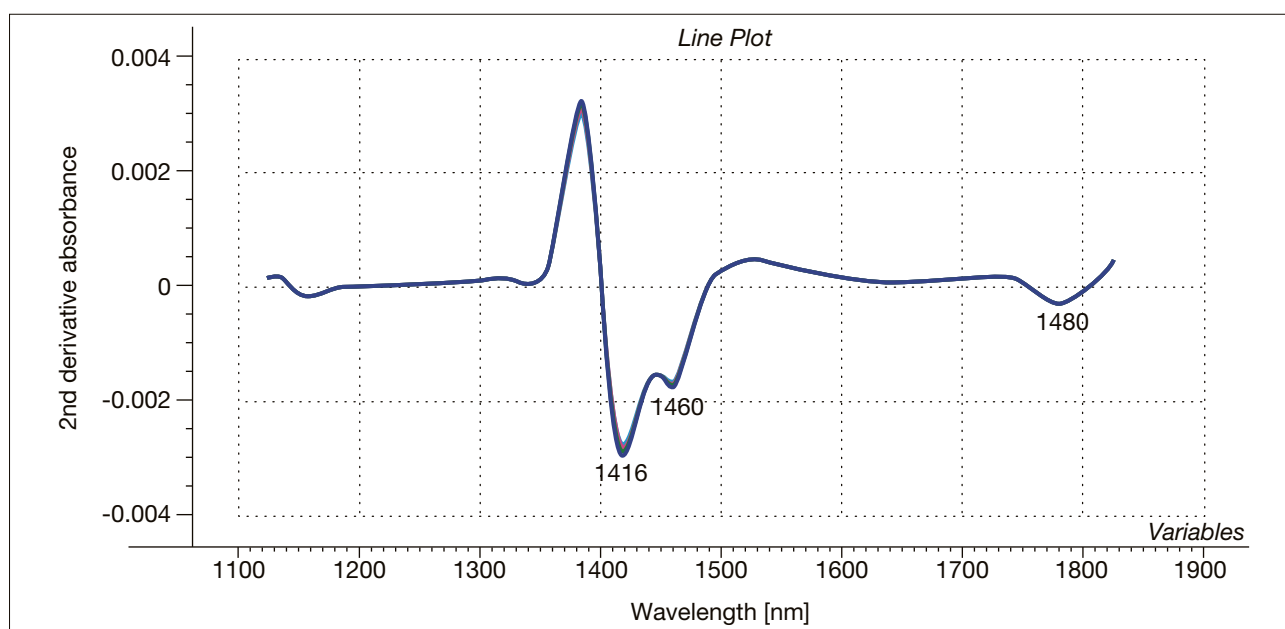


Figure 2. Second derivative spectra of the sugar solutions in the range of 1100-1850 nm

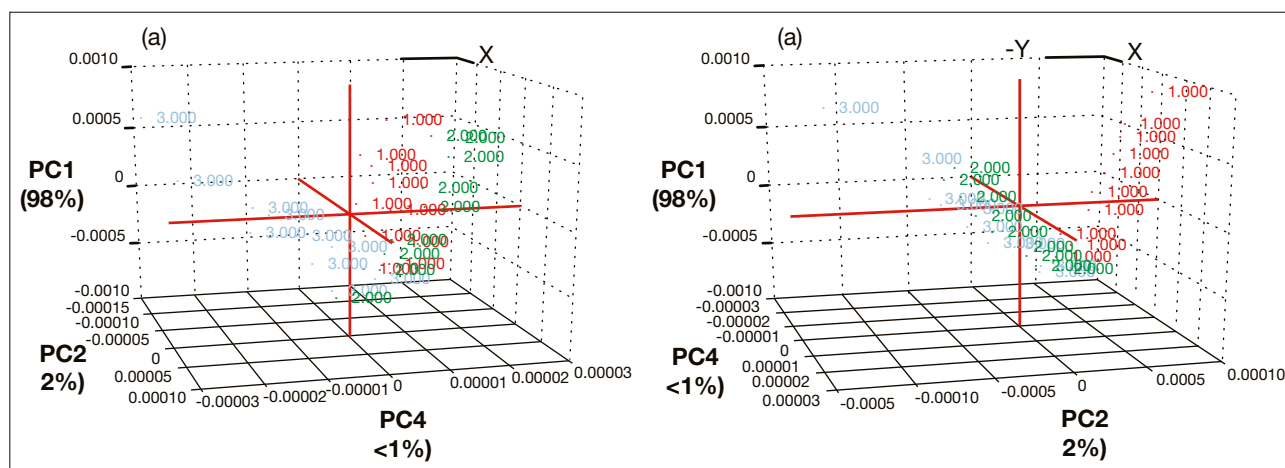
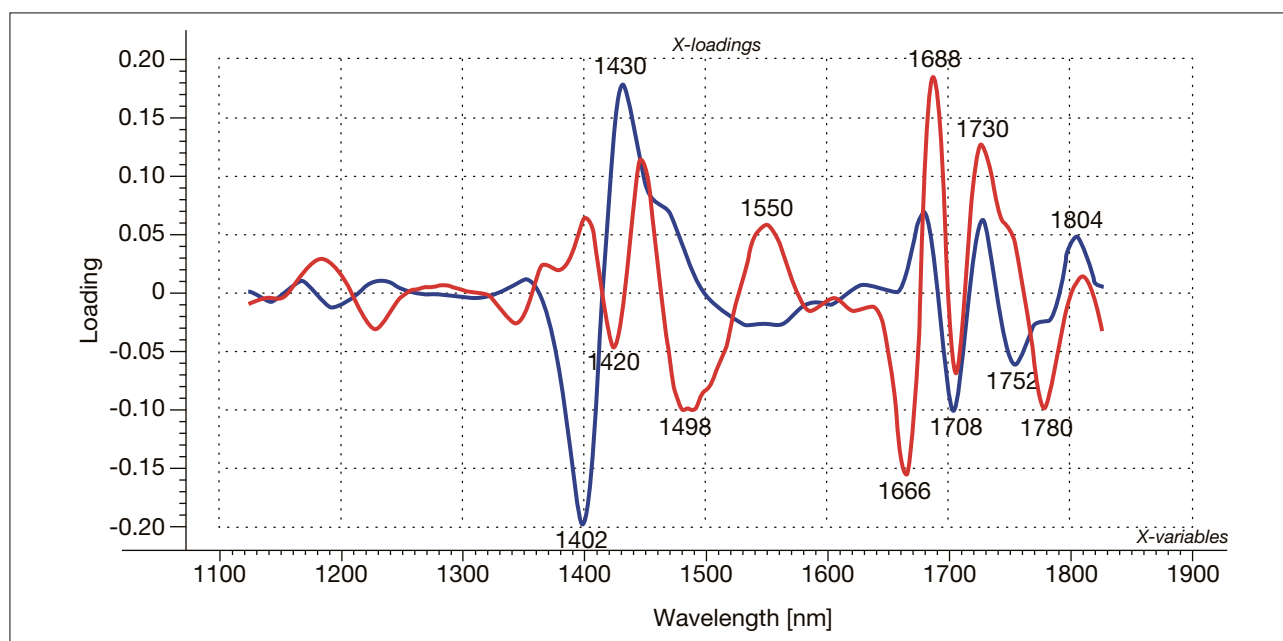


Figure 3. 3D plots of the principal component analysis (PCA) of the three types of sugar solutions using 2<sup>nd</sup> derivative spectra, showing (a) the 1<sup>st</sup> principal component (PC1), PC2 and PC4, and (b) PC1, PC4 and PC2. The red (1), green (2) and light blue (3) scores represent D-sucrose, K-Syrup LDX, and K-Sweet F55, respectively.

**Figure 4** shows the loading vectors of PC2 and PC4. The wavelength regions having the largest deviation from zero are the most responsible for score values of the principal components, thus, the assigned peaks indicate the absorptions causing the difference between the sugar solutions. The band assignments are in good harmony with previous findings [14], [15], i.e. peaks in the 1300-1600 nm interval refer to the molecular changes of water caused by the dissolved sugars, while the peaks in the 1600-1850 nm interval represent characteristic C–H bands.

The results of the calibration models developed using PLS regression on the measured °Brix and calculated fructose, glucose, sucrose concentrations are presented in **Table 2** and **Figure 5**.



*Figure 4. The loading vectors of PC2 and PC4 showing the absorption bands responsible for the separation of D-sucrose from K-Syrup LDX and K-Sweet F55, and for the separation of K-Sweet F55 from D-sucrose and K-Syrup LDX, respectively*

*Table 2. The calibration and cross-validation statistics for °Brix, glucose, fructose and sucrose concentration in the sugar solutions (n = 30), highlighting the best model for each*

Math treatment	LV	Constituent	R <sup>2</sup> <sub>c</sub>	RMSEC (g/100ml)	R <sup>2</sup> <sub>cv</sub>	RMECV (g/100ml)
NONE	1	°Brix	0.846	1.06	0.842	1.09
NONE	3	Fructose	0.921	0.33	0.831	0.51
NONE	3	Glucose	0.871	0.85	0.820	1.04
NONE	3	Sucrose	0.927	0.83	0.897	1.02
MSC	1	°Brix	0.853	1.04	0.832	1.10
MSC	3	Fructose	0.791	0.47	0.573	0.70
MSC	3	Glucose	0.942	0.58	0.907	0.78
MSC	3	Sucrose	0.976	0.50	0.958	0.58
SNV	1	°Brix	0.857	1.01	0.794	1.26
SNV	3	Fructose	0.750	0.55	0.642	0.70
SNV	3	Glucose	0.914	0.68	0.868	0.88
SNV	3	Sucrose	0.962	0.60	0.936	0.81
2D5G5S	2	°Brix	0.861	1.00	0.823	1.15
2D5G5S	3	Fructose	0.772	0.51	0.648	0.64
2D5G5S	3	Glucose	0.954	0.50	0.907	0.74
2D5G5S	2	Sucrose	0.982	0.40	0.976	0.51

*LV: number of latent variables, R<sup>2</sup><sub>c</sub>: determination coefficient of calibration, RMSEC: root mean square error of calibration, R<sup>2</sup><sub>cv</sub>: determination coefficient of cross-validation, RMSECV: root mean square error of cross-validation, MSC: multiplicative scatter correction, SNV: standard normal variate, 2D5G5S: 2nd order derivative with 5-point gap and 5-point segment*



The best results for °Brix were achieved with no spectral pretreatment. The RMSE of °Brix remained around 1 °Bx, which was almost third of the standard deviation of the measured reference values. The RMSE of the sugar concentrations was similarly low. The least accurate model was achieved for fructose, which is caused by the group of samples with fructose content below 0.05% - for these samples the model performed worse than in the higher concentration regions (**Figure 5. (b)**). Second derivative pretreatment gave the best result for glucose and sucrose, while the best models for fructose were achieved without pretreatment of the NIR spectra.

The calibration and cross-validation regression lines (Y-fit) of the best °Brix, fructose, glucose and sucrose models are shown in **Figure 5**. The black diagonal line shows the optimal Y-fit, while blue and red lines show the calibration and cross-validation Y-fits. The blue dots show the NIR predicted composition values of samples during calibration in the function of the laboratory reference values, and red dots show the NIR predicted values at cross-validation testing, again, in the function of the reference values measured. The closer the dots are to the regression line and the less the regression line deviates from the optimal Y-fit, the better the calibration model is. In most of the cases, the achieved Y-fits are hitting the optimum, meaning that the NIR predicted values are almost equal to the actual laboratory reference values. The calibration and cross-validation results of this study are in agreement with the previously cited results achieved with sugar solutions and fruit juices. These results confirm that, after a proper calibration process, NIR spectroscopy is a useful and effective tool for easy, rapid and accurate measurement of individual sugars in mixed solutions.

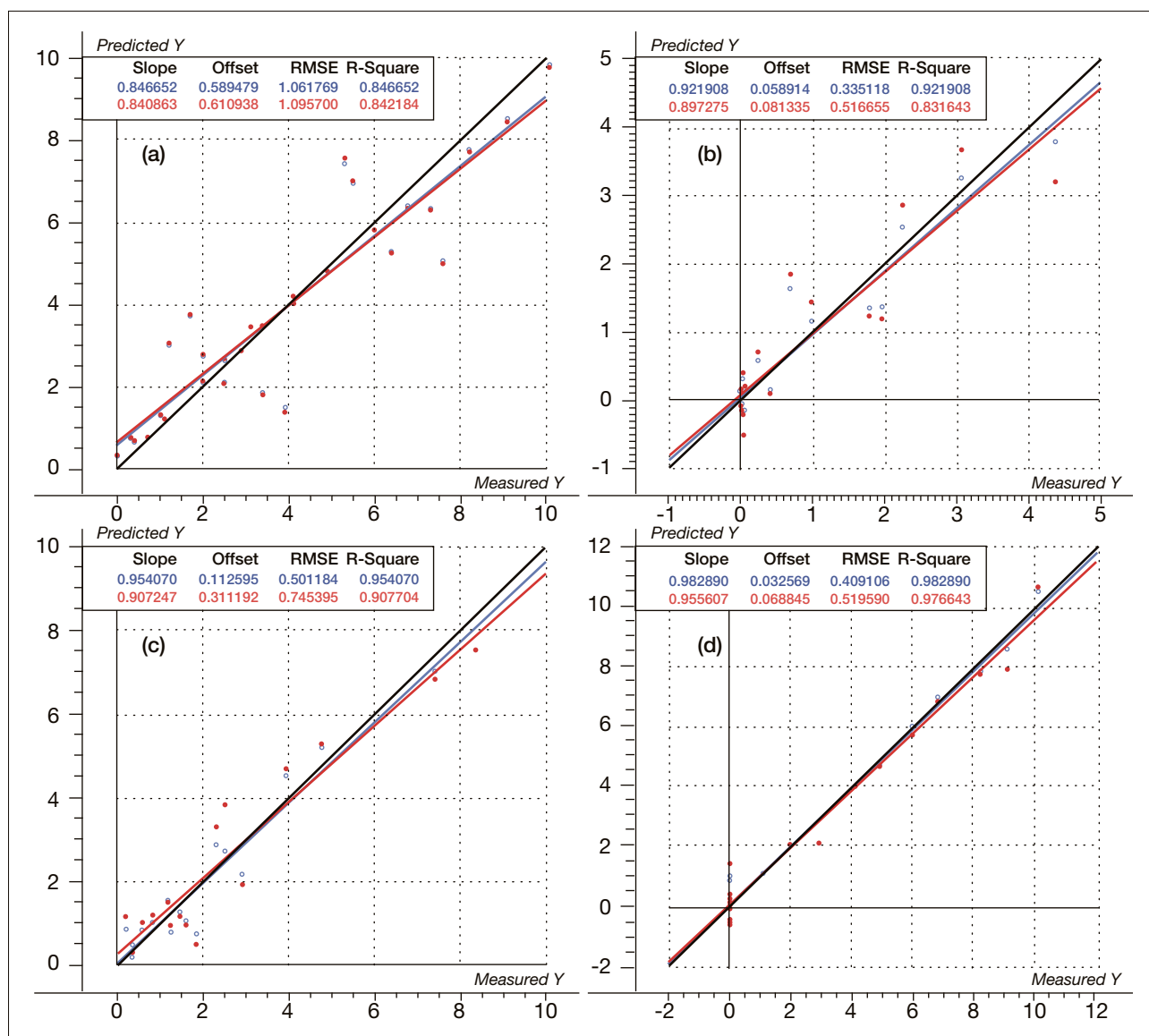


Figure 5. The optimum Y-fit (black diagonal) and the Y-fits of the best calibrations (blue) and cross-validations (red) for (a) °Brix, concentration of (b) fructose, (c) glucose and (d) sucrose



## 5. Conclusions

The results of this study performed with widely used sweeteners confirm the previously published findings that NIR spectroscopy is a useful and powerful technology to detect and quantify individual sugar types even in mixture solutions. Since NIR spectrometers have not only reached the portable size but have become extremely small as a fingernail-sized chip, the importance of this technology in everyday food qualification seems to be underestimated. Wide aspects of applications should be tested and used for monitoring products and warrant food safety and quality. Among these applications, checking and certifying the fructose content of beverages and foods would advantage consumers' health, as this constituent has been proven to raise the risk of several diseases of modern times. NIR spectroscopy as secondary correlative analytical technology will likely remain to be unsuitable for detecting and quantifying fructose in a complex liquid of completely unknown composition, but may be suitable for indicating the excessive presence of fructose in a known liquid meant to be containing no or only a certain amount of fructose. The usability of NIR tools is limited and they should not be considered as substitutes of classical analytical methods, however, by rational use of opportunities, useful applications can be developed for practice.

## 6. References

- [1] Edwards, C. H., Rossi, M., Corpe, C. P., Butterworth, P. J., & Ellis, P. R. (2016): The role of sugars and sweeteners in food, diet and health: Alternatives for the future. *Trends in Food Science and Technology*, 56, pp. 158-166.  
<https://doi.org/10.1016/j.tifs.2016.07.008>
- [2] White, E., McMahon, M., Walsh, M., Coffey, J. C., & O'Sullivan, L. (2014): Creating Biofidelic Phantom Anatomies of the Colorectal Region for Innovations in Colorectal Surgery. *Proceedings of the International Symposium on Human Factors and Ergonomics in Health Care*, 3 (1), pp. 277-282.  
<https://doi.org/10.1177/2327857914031045>
- [3] Gardner, C., Wylie-Rosett, J., Gidding, S. S., Steffen, L. M., Johnson, R. K., Reader, D., & Lichtenstein, A. H. (2012): Nonnutritive sweeteners: Current use and health perspectives: A scientific statement from the American heart association and the American diabetes association. *Circulation*, 126 (4), pp. 509-519.  
<https://doi.org/10.1161/CIR.0b013e31825c42ee>
- [4] Taskinen, M. R., Packard, C. J., & Borén, J. (2019): Dietary fructose and the metabolic syndrome. *Nutrients*, 11 (9), pp. 1-16.  
<https://doi.org/10.3390/nu11091987>
- [5] Bray, G. A. (2013): Energy and fructose from beverages sweetened with sugar or high-fructose corn syrup pose a health risk for some people. *Advances in Nutrition*, 4 (2), pp. 220-225.  
<https://doi.org/10.3945/an.112.002816>
- [6] Malik, V. S., & Hu, F. B. (2015): Fructose and Cardiometabolic Health What the Evidence from Sugar-Sweetened Beverages Tells Us. *Journal of the American College of Cardiology*, 66 (14), pp. 1615-1624.  
<https://doi.org/10.1016/j.jacc.2015.08.025>
- [7] Rizkalla, S. W. (2010): Health implications of fructose consumption: A review of recent data. *Nutrition and Metabolism*, 7, pp. 1-17.  
<https://doi.org/10.1186/1743-7075-7-82>
- [8] Biró, G. (2018): Human biological characteristics of fructose. *Journal of Food Investigation*, 64 (1), pp. 1908-1916.
- [9] Collino, M. (2011): High dietary fructose intake: Sweet or bitter life? *World Journal of Diabetes*, 2 (6), pp. 77.  
<https://doi.org/10.4239/wjd.v2.i6.77>
- [10] Liu, Y., Ying, Y., Yu, H., & Fu, X. (2006): Comparison of the HPLC method and FT-NIR analysis for quantification of glucose, fructose, and sucrose in intact apple fruits. *Journal of Agricultural and Food Chemistry*, 54 (8), pp. 2810-2815.  
<https://doi.org/10.1021/jf052889e>
- [11] Giannoccaro, E., Wang, Y. J., & Chen, P. (2008): Comparison of two HPLC systems and an enzymatic method for quantification of soybean sugars. *Food Chemistry*, 106 (1), pp. 324-330.  
<https://doi.org/10.1016/j.foodchem.2007.04.065>
- [12] Yuan, H., Wu, Y., Liu, W., Liu, Y., Gao, X., Lin, J., & Zhao, Y. (2015): Mass spectrometry-based method to investigate the natural selectivity of sucrose as the sugar transport form for plants. *Carbohydrate Research*, 407, pp. 5-9.  
<https://doi.org/10.1016/j.carres.2015.01.011>
- [13] International Association of Analytical Chemistry, A. (1990): *Official Methods of Analysis of the AOAC*. Arlington VA

- [14] López, M. G., García-González, A. S., & Franco-Robles, E. (2017): Carbohydrate Analysis by NIRS-Chemometrics. In K. G. Kyrianiadis & S. Jan (Eds.), *Developments in Near-Infrared Spectroscopy* pp. 81-95  
<https://doi.org/10.5772/67208>
- [15] Bázár, G., Kovacs, Z., Tanaka, M., Furukawa, A., Nagai, A., Osawa, M., Itakura, Y., Sugiyama, H., Tsenkova, R. (2015): Water revealed as molecular mirror when measuring low concentrations of sugar with near infrared light. *Analytica Chimica Acta*, 896, pp. 52-62.  
<https://doi.org/10.1016/j.aca.2015.09.014>
- [16] Xie, L., Ye, X., Liu, D., & Ying, Y. (2009): Quantification of glucose, fructose and sucrose in bayberry juice by NIR and PLS. *Food Chemistry*, 114 (3), pp. 1135-1140.  
<https://doi.org/10.1016/j.foodchem.2008.10.076>
- [17] Rodriguez-Saona, L. E., Fry, F. S., McLaughlin, M. A., & Calvey, E. M. (2001): Rapid analysis of sugars in fruit juices by FT-NIR spectroscopy. *Carbohydrate Research*, 336 (1), pp. 63-74.  
[https://doi.org/10.1016/S0008-6215\(01\)00244-0](https://doi.org/10.1016/S0008-6215(01)00244-0)
- [18] Mekonnen, B. K., Yang, W., Hsieh, T. H., Liaw, S. K., & Yang, F. L. (2020): Accurate prediction of glucose concentration and identification of major contributing features from hardly distinguishable near-infrared spectroscopy. *Biomedical Signal Processing and Control*, 59, pp. 101923.  
<https://doi.org/10.1016/j.bspc.2020.101923>
- [19] De Oliveira, V. M. A. T., Baqueta, M. R., Março, P. H., & Valderrama, P. (2020): Authentication of organic sugars by NIR spectroscopy and partial least squares with discriminant analysis. *Analytical Methods*, 12, pp. 701-705.  
<https://doi.org/DOI: 10.1039/C9AY02025J>
- [20] Khadem, H., Eissa, M. R., Nemat, H., Alrezj, O., & Benaissa, M. (2020): Classification before regression for improving the accuracy of glucose quantification using absorption spectroscopy. *Talanta*, 211 (January), pp. 120740.  
<https://doi.org/10.1016/j.talanta.2020.120740>
- [21] Hao, Q., Zhou, J., Zhou, L., Kang, L., Nan, T., Yu, Y., & Guo, L. (2020): Prediction the contents of fructose, glucose, sucrose, fructo-oligosaccharides and iridoid glycosides in *Morinda officinalis* radix using near-infrared spectroscopy. *Spectrochimica Acta - Part A: Molecular and Biomolecular Spectroscopy*, pp. 234  
<https://doi.org/10.1016/j.saa.2020.118275>
- [22] KALL, I. (2020): K-syrup LDX. Retrieved from <http://kallingredients.hu/en/products/2/14/k-syrup-ldx>
- [23] KALL, I. (2020): K-sweet F55. Retrieved from <http://kallingredients.hu/en/products/2/12/k-sweet>
- [24] Naes, T., Isaksson, T., Fearn, T., & Davies, T. (2002): *A user-friendly guide to multivariate calibration and classification*. Chichester, UK: NIR Publications